

# Synthesis of Ruthenium Complexes Bearing PCP-Type Pincer Ligands and Their Application to Direct Synthesis of Imines from Amines and Benzyl Alcohol

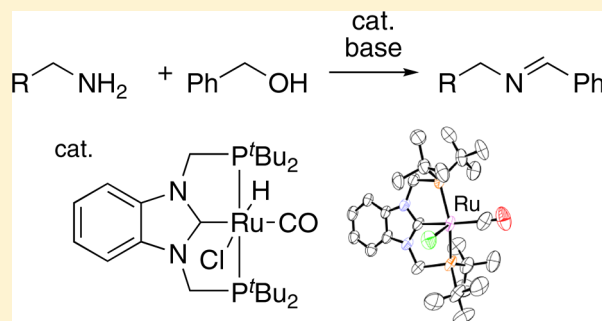
Aya Eizawa,<sup>†</sup> Shunsuke Nishimura,<sup>†</sup> Kazuya Arashiba,<sup>†</sup> Kazunari Nakajima,<sup>‡</sup> and Yoshiaki Nishibayashi<sup>\*,†</sup>

<sup>†</sup>Department of Systems Innovation, School of Engineering, The University of Tokyo, Bunkyo-ku, Tokyo 113-8656, Japan

<sup>‡</sup>Frontier Research Center for Energy and Resources, School of Engineering, The University of Tokyo, Bunkyo-ku, Tokyo 113-8656, Japan

## Supporting Information

**ABSTRACT:** Ruthenium complexes bearing *N*-heterocyclic carbene- and phosphine-based PCP-type pincer ligands are synthesized and characterized by X-ray crystallography. The ruthenium–PCP complexes have catalytic activity toward direct synthesis of imines from reactions of amines and benzyl alcohol. The lifetime of the ruthenium complex bearing the PCP pincer ligand is longer than that of the ruthenium complex bearing a pyridine-based PNP-type pincer ligand.



## INTRODUCTION

Pincer-type ligands, which bind to metal in a meridional fashion, are essential in modern organic and inorganic chemistry.<sup>1</sup> In particular, transition-metal complexes bearing a pyridine-based PNP-type pincer ligand have enabled a wide range of salient catalytic reactions, where the PNP ligand usually worked as a noninnocent ligand via deprotonation of a methylene hydrogen atom at the benzylic position of the pyridine ring.<sup>2</sup> For example, ruthenium-, iridium-, and cobalt–PNP complexes catalytically promoted dehydrogenation of alcohols,<sup>3–5</sup> hydrogenation of carbon dioxide,<sup>6</sup> and C–H borylation of arenes and heterocycles,<sup>7</sup> respectively (Figure 1a).

In 2011, we found that molybdenum–PNP complexes worked as an effective catalyst toward reduction of dinitrogen into ammonia under ambient reaction conditions (Figure 1b).<sup>8,9</sup> As part of an extensive study, we designed and synthesized two kinds of *N*-heterocyclic carbene- and phosphine-based PCP-type pincer ligands, namely PCP[1] and PCP[2] ligands (PCP[1] = 1,3-bis((di-*tert*-butylphosphino)methyl)benzimidazol-2-ylidene; PCP[2] = 1,3-bis(2-(di-*tert*-butylphosphino)ethyl)imidazol-2-ylidene), because both of the PCP ligands are expected to have strong electron-donating and -coordinating ability at the metal center.<sup>10,11</sup> The *N*-heterocyclic carbene (NHC)<sup>12</sup> unit and the two phosphine units of PCP[1] and PCP[2] are connected with methylene and ethylene linkers, respectively.

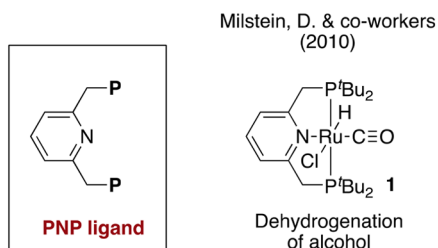
Interestingly, dinitrogen-bridged dimolybdenum complex bearing PCP[1] ligands [ $\{\text{Mo}(\text{N}_2)_2(\text{PCP}[1])\}_2(\mu\text{-N}_2)$ ]

worked as effective catalysts toward reduction of dinitrogen into ammonia under ambient reaction conditions (Figure 1b). The amount and the rate of ammonia production were higher than those of dinitrogen-bridged dimolybdenum complex bearing PNP ligands [ $\{\text{Mo}(\text{N}_2)_2(\text{PNP})\}_2(\mu\text{-N}_2)$ ] (PNP = 2,6-bis(di-*tert*-butylphosphinomethyl)pyridine). In contrast to the molybdenum–PCP[1] complex, a dinitrogen-bridged dimolybdenum complex bearing PCP[2] ligands [ $\{\text{Mo}(\text{N}_2)_2(\text{PCP}[2])\}_2(\mu\text{-N}_2)$ ] had no catalytic activity toward reduction of dinitrogen into ammonia under the same reaction conditions. We consider that dinuclear structure is an essential factor to promote the catalytic reaction; however, the steric hindrance of the PCP[2] ligand did not allow its dinuclear structure to be maintained in solution.<sup>10</sup>

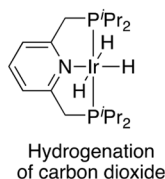
The superior activity and stability of molybdenum–PCP complexes prompted us to explore the potential of the PCP–pincer ligands in other transition-metal-catalyzed reactions.<sup>13</sup> We have focused on the unique catalytic activity of ruthenium–PNP complexes toward dehydrogenative transformations of alcohols. For example, Milstein and co-workers reported direct preparation of imines from reactions of amines with alcohols in the presence of a catalytic amount of  $[\text{RuHCl}(\text{CO})(\text{PNP})]$  (**1**).<sup>4c</sup> Herein, we report the preparation of ruthenium complexes bearing PCP[1] and PCP[2] ligands  $[\text{RuHCl}(\text{CO})(\text{PCP})]$  (**2a**, PCP = PCP[1]; **2b**, PCP = PCP[2]) and their catalytic application (Figure 1c).

**Received:** July 5, 2018

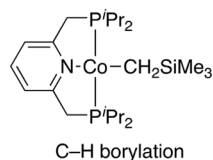
## a) Previous works : transition metal–PNP complexes



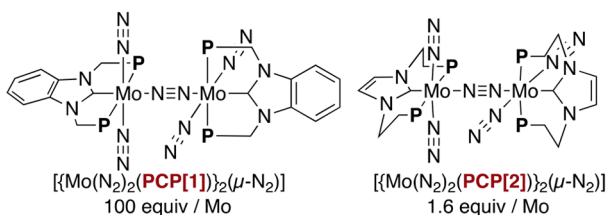
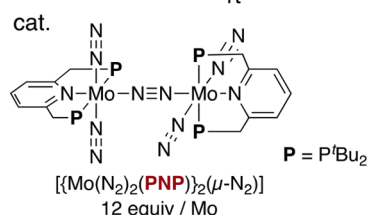
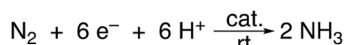
Nozaki, K. &amp; co-workers (2009)



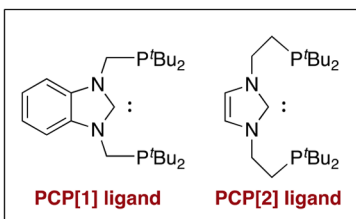
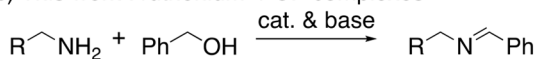
Chirik, P. J. &amp; co-workers (2014)



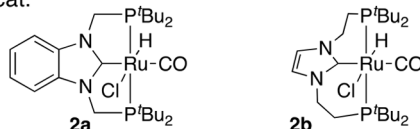
## b) Our previous works : dimolybdenum–dinitrogen complexes bearing PNP or PCP ligands



## c) This work : ruthenium–PCP complexes



cat.



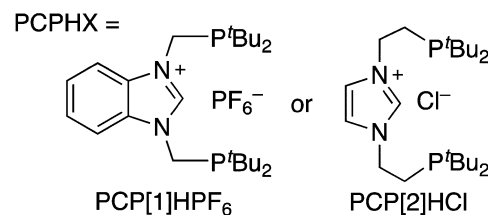
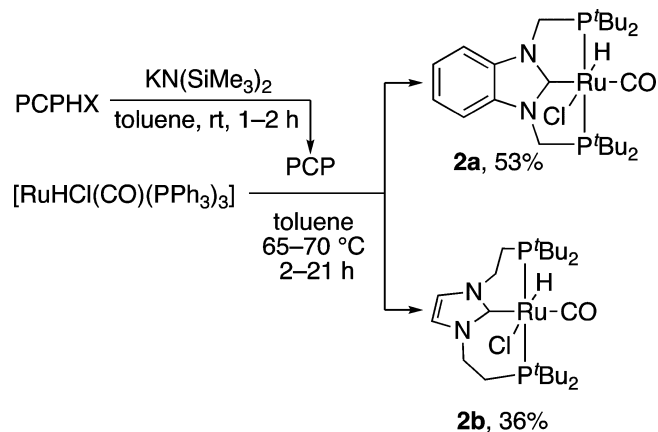
Ruthenium–PCP complexes

**Figure 1.** Transition metal–pincer complexes. (a) Transition metal–PNP complexes (b) Dimolybdenum–dinitrogen complexes bearing PNP or PCP ligands. (c) Ruthenium complexes bearing PCP[1] and PCP[2] ligands.

## RESULTS AND DISCUSSION

Reactions of  $[\text{RuHCl}(\text{CO})(\text{PPh}_3)_3]$  with PCP ligands, generated in situ from the corresponding imidazolium salts with 1.4 equiv of  $\text{KN}(\text{SiMe}_3)_2$ , in toluene under heating reaction conditions afforded ruthenium complexes bearing a PCP ligand  $[\text{RuHCl}(\text{CO})(\text{PCP})]$  **2a** and **2b** in 53% yield and 36% yield, respectively (Scheme 1). The ruthenium complexes

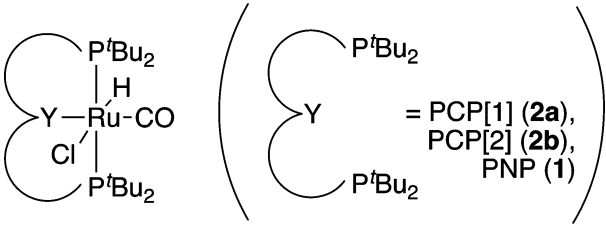
## Scheme 1. Synthesis of Ruthenium–PCP Complexes 2



were characterized by NMR, IR, and elemental analysis. In the  $^1\text{H}$  NMR spectra of complexes **2a** and **2b**, triplet signals were observed at  $-16.84$  and  $-17.43$  ppm, respectively. These signals indicate the hydride ligand on the ruthenium atoms. This result is supported by the IR absorptions of complexes **2a** and **2b** at  $2109$  and  $2046 \text{ cm}^{-1}$  assignable to the hydride ligands, respectively.

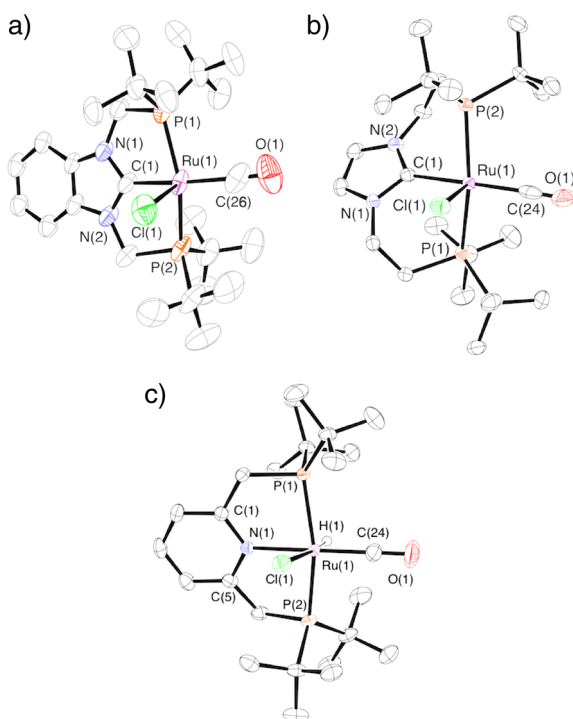
On the other hand, IR spectra of **2a** and **2b** showed a band assignable to the carbonyl ligand at  $1937$  and  $1907 \text{ cm}^{-1}$ , respectively (Table 1). This result indicates that a remarkable difference was observed, although benzimidazol-1-ylidene of PCP[1] ligand and imidazole-1-ylidene of PCP[2] ligand have a similar electron-donating ability.<sup>10,14</sup> The higher frequency of the carbonyl ligand in **2a** is linked to stronger  $\pi$ -accepting characters of the PCP[1] ligand compared to that of the PCP[2] ligand. This tendency of the ruthenium complexes is consistent with that of the dinitrogen-bridged dimolybdenum complexes.<sup>10</sup> For comparison, the IR spectrum of **1** showed a band assignable to the carbonyl ligand at  $1906 \text{ cm}^{-1}$ .<sup>4c</sup>

Detailed molecular structures of both complexes are confirmed by X-ray analysis. ORTEP drawings of **2a** and **2b** are shown in parts a and b, respectively, of Figure 2. Representative bond lengths and dihedral angles are shown in Table 1. The crystal structures of **2a** and **2b** display distorted octahedral geometries around the ruthenium centers. The carbonyl ligands occupy the position *trans* to the NHC unit of PCP ligand with the hydride and chloride ligands located *trans* to each other. Bond lengths of  $\text{Ru}(1)\text{--C}(1)$  in **2a** and **2b** were  $2.011(6)$  and  $2.087(3) \text{ \AA}$ , respectively. The

**Table 1. Structural Parameters of Ruthenium Complexes 2a, 2b, and 1**


	2a	2b	1
$\nu_{\text{CO}}$ ( $\text{cm}^{-1}$ )	1937	1907	1906 <sup>a</sup>
Ru–Y ( $\text{\AA}$ )	2.011(6)	2.087(3)	2.1438(13)
Dihedral angles ( $^{\circ}$ ) <sup>b</sup>	76.64	43.44	70.92
Ru–CO ( $\text{\AA}$ )	1.938(9)	1.939(5)	1.8389(18)

<sup>a</sup>Reference 4c. <sup>b</sup>NHC or pyridine and Cl–Ru–Y plane.

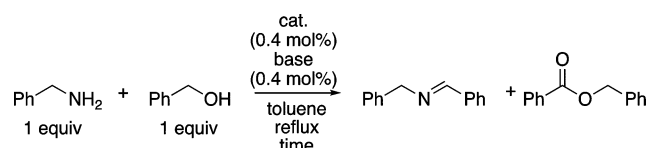
**Figure 2.** ORTEP drawings of ruthenium–PCP and PNP complexes **2a**, **2b**, and **1**. Thermal ellipsoids are shown at the 50% probability level. All of the hydrogen atoms except for H(1) atom of **1** are omitted for clarity. (a) ORTEP drawing of **2a**. Minor disorder components of complex **2a** are omitted for clarity. (b) ORTEP drawing of **2b**. (c) ORTEP drawing of **1**.

significantly shorter bond length between Ru(1)–C(1) of **2a** than that of **2b** also suggests stronger  $\pi$ -back-donation from the ruthenium atom to the NHC unit. The dihedral angles defined by N(1)–C(1)–N(2) and Cl(1)–Ru(1)–C(1) planes of **2a** and **2b** were 76.64° and 43.44°, respectively. The dihedral angle of **2a** enables effective overlapping between d

orbital of the ruthenium atom and the empty p orbital of the carbon atom.<sup>10</sup>

For comparison, we have newly analyzed PNP complex **1** with X-ray crystallography. An ORTEP drawing of **1** is shown in Figure 2c. The coordination geometry of **1** is similar to that of **2**. The bond length between Ru(1)–N(1) of **1** was 2.1438(13) Å. The dihedral angle defined by C(1)–N(1)–C(5) and Cl(1)–Ru(1)–N(1) planes was 70.92°. The bond length between Ru(1)–CO of **1** was significantly shorter than those of **2a** or **2b**, implying stronger trans influence of NHCs of the PCP ligands than the pyridine of the PNP ligand (1.8389(18) Å for **1**, 1.938(9) Å for **2a**, and 1.939(5) Å for **2b**, Table 1).

With the novel ruthenium complexes bearing PCP ligands in hand, we carried out catalytic formation of an imine from the reaction of benzylamine with benzyl alcohol, following the previous reaction conditions by Milstein<sup>4c</sup> and our group.<sup>15</sup> The reaction of benzylamine with 1 equiv of benzyl alcohol in the presence of 0.4 mol % of **2a** and sodium isopropoxide (NaO<sup>t</sup>Pr) in toluene at a reflux temperature for 48 h gave *N*-benzylidenebenzylamine in 86% yield (Table 2, run 1). The

**Table 2. Catalytic Formation of Imine from Benzylamine and Benzyl Alcohol with Catalyst 2 or 1 and Base<sup>a</sup>**


run	catalyst	base	time (h)	yield of imine <sup>b</sup> (%)	yield of ester <sup>b</sup> (%)
1	2a	NaO <sup>t</sup> Pr	48	86	trace
2	2b	NaO <sup>t</sup> Pr	48	70	trace
3	1	NaO <sup>t</sup> Pr	48	69	6
4	2a	NaO <sup>t</sup> Pr	24	63	0
5	1	NaO <sup>t</sup> Pr	24	69	6
6	2a	KO <sup>t</sup> Bu	24	60	trace
7	1	KO <sup>t</sup> Bu	24	46	11
8 <sup>c</sup>	2a	NaO <sup>t</sup> Pr	24	52	0
9 <sup>c</sup>	1	NaO <sup>t</sup> Pr	24	27	0
10	none	NaO <sup>t</sup> Pr	24	trace	0
11	2a	none	24	24	0
12	1	none	24	7	0

<sup>a</sup>Reactions of benzylamine (5.0 mmol) with benzyl alcohol (5.0 mmol) were carried out in the presence of Ru catalyst (0.02 mmol) and base (0.02 mmol) in toluene (1 mL) at reflux temperature. <sup>b</sup>NMR yield. Hexamethylbenzene was used as an internal standard. <sup>c</sup>Catalyst (0.2 mol %) and base (0.2 mol %) were used.

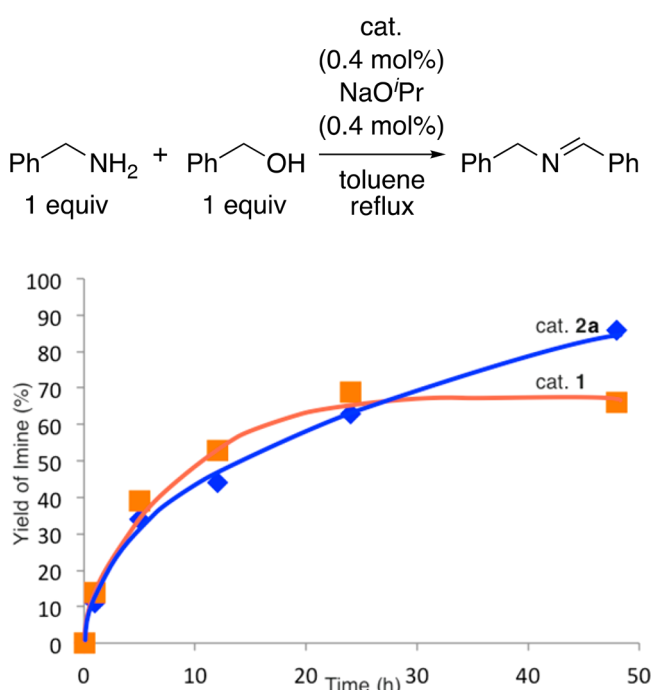
use of **2b** as a catalyst under the same reaction conditions gave the same imine in 70% yield (Table 2, run 2). For comparison, when complex **1** was used as a catalyst, the imine was obtained in 69% together with benzyl benzoate in 6% as a byproduct (Table 2, run 3). These results indicate that complex **2a** shows the best performance in the present reaction.

In the following runs, we compared the catalytic activity of **2a** with that of **1**. When the catalytic reaction was carried out for a shorter reaction time of 24 h, the imine was obtained in 63% and 69% yields, respectively (Table 2, runs 4 and 5). The use of potassium *tert*-butoxide (KO<sup>t</sup>Bu) in place of NaO<sup>t</sup>Pr as a base afforded the imine in lower yields, in both cases (Table 2, runs 6 and 7). In the presence of 0.2 mol % of the catalyst and

NaO<sup>t</sup>Pr, a slightly lower yield of the imine was observed when complex **2a** was used (Table 2, run 8). In contrast, less than half amount of the imine was obtained when complex **1** was used (Table 2, run 9). These experimental results indicate that the catalytic activity of **2a** is higher than that of **1** under the same reaction conditions. Separately, we investigated some control experiments (Table 2, runs 10–12). The combination of ruthenium complex and base is an essential factor to promote the catalytic reaction.

Next, we monitored the time profile of catalytic reactions using **2a** and **1** as catalysts under the same reaction conditions. Typical results are shown in Scheme 2. At the beginning of the

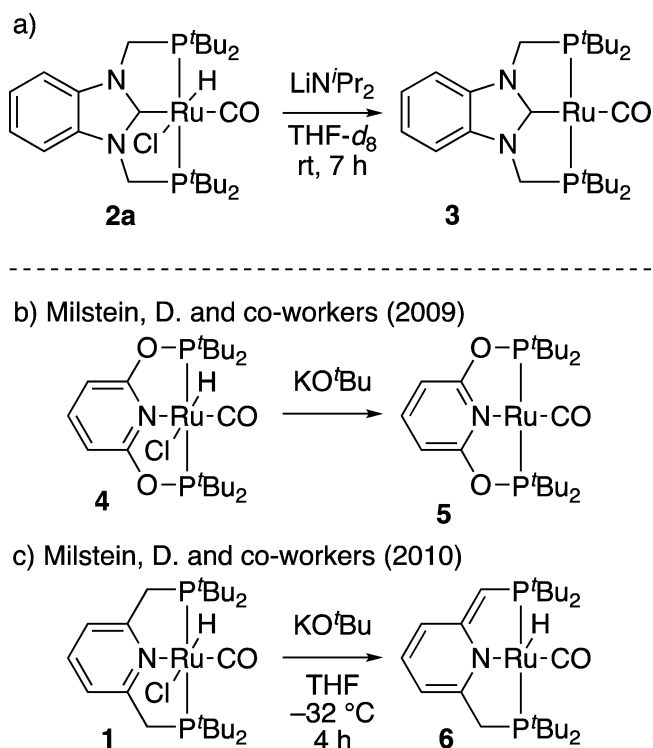
**Scheme 2. Time Profile of Synthesis of Imine Catalyzed by **2a** and **1****



reaction, the amount of the produced imine in the case of **2a** was slightly lower than that of **1**. After 48 h from the beginning of the reactions, however, the amount of imine in the case of **2a** was substantially higher than that of **1**. In the reaction using **1** as a catalyst, no further production of imine was observed after 24 h from the beginning of catalytic reaction. We consider that the lifetime of complex **2a** is longer than that of complex **1** under the present reaction conditions. The longer lifetime of **2a** is supposed to be because of the strong  $\pi$ -accepting property of PCP[1] ligand, which leads large bond energy between ruthenium atom and PCP[1] ligand.

In order to obtain further information on the reaction mechanism, we carried out the following stoichiometric reaction of **2a**. After treatment of **2a** with 1 equiv of lithium diisopropylamide ( $\text{LiN}^i\text{Pr}_2$ ) in THF- $d_8$  at room temperature for 7 h, formation of another complex was observed by NMR (Scheme 3a). This complex was also characterized by IR. No signals for hydride ligand appeared in the NMR spectrum. The IR spectrum showed a band assignable to carbonyl ligand at  $1845\text{ cm}^{-1}$ , which is much lower frequency than that of **2a**. Based on these NMR and IR spectra, we identified this novel complex as a square-planar ruthenium(0) carbonyl complex  $[\text{Ru}(\text{CO})(\text{PCP}[1])]$  (**3**). A similar square-planar ruthenium(0) carbonyl complex was reported from the reaction of ruthenium–PONOP complex  $[\text{RuHCl}(\text{CO})(\text{PONOP})]$  (**4**; PONOP = 2,6-bis((di-*tert*-butylphosphanyl)oxy)pyridine) with 1 equiv of  $\text{KO}^t\text{Bu}$  to give the corresponding square-planar ruthenium(0) carbonyl complex  $[\text{Ru}(\text{CO})(\text{PONOP})]$  (**5**) (Scheme 3b).<sup>16</sup>

**Scheme 3. Stoichiometric Reactions of Ruthenium Complexes with Base**



These stoichiometric reactions shown in Scheme 3a,b are in sharp contrast to the reaction of  $[\text{RuHCl}(\text{CO})(\text{PNP})]$  **1** with 1 equiv of  $\text{KO}^t\text{Bu}$  to give a ruthenium(II) amide complex (**6**) (Scheme 3c).<sup>4c</sup> In this case, deprotonation of a hydrogen atom at the benzylic position of the pyridine ring proceeded to give the corresponding unsaturated complex **6**. Milstein and co-workers previously proposed that the unsaturated amide complex **6** plays a key role of the catalytic transformation.<sup>4c</sup>

We investigated catalytic reactions of other amines with benzyl alcohol using **2a** and **1** as catalysts. Reactions of *n*-hexylamine and cyclohexylamine with 1 equiv of benzyl alcohol in the presence of 0.4 mol % of **2a** and sodium isopropoxide ( $\text{NaO}^i\text{Pr}$ ) in toluene at reflux temperature afforded *N*-benzylidenehexylamine and *N*-benzylidenecyclohexylamine in 75% and 72% yields, respectively (Scheme 4). For comparison, when **1** was used in place of **2a**, the same imines were obtained in 46% and 62% yields, respectively (Scheme 4). These results indicate that complex **2a** worked as a more effective catalyst than complex **1** under the present reaction conditions.

On the basis of the experimental results, we have proposed a plausible reaction pathway as shown in Figure 3. First, the reaction of **2a** with 1 equiv of  $\text{NaO}^i\text{Pr}$  gives the square-planar ruthenium(0) complex  $[\text{Ru}(\text{CO})(\text{PCP}[1])]$  **3**, which undergoes oxidative addition of benzyl alcohol to give the corresponding alkoxide and hydride complex (**A**). Then,  $\beta$ -hydride elimination affords benzaldehyde complex (**B**) together with dissociation of one di-*tert*-butylphosphino group on the PCP[1] ligand. Subsequent dissociation of



## Scheme 4. Catalytic Formation of Imines from Reactions of Amines with Benzyl Alcohol

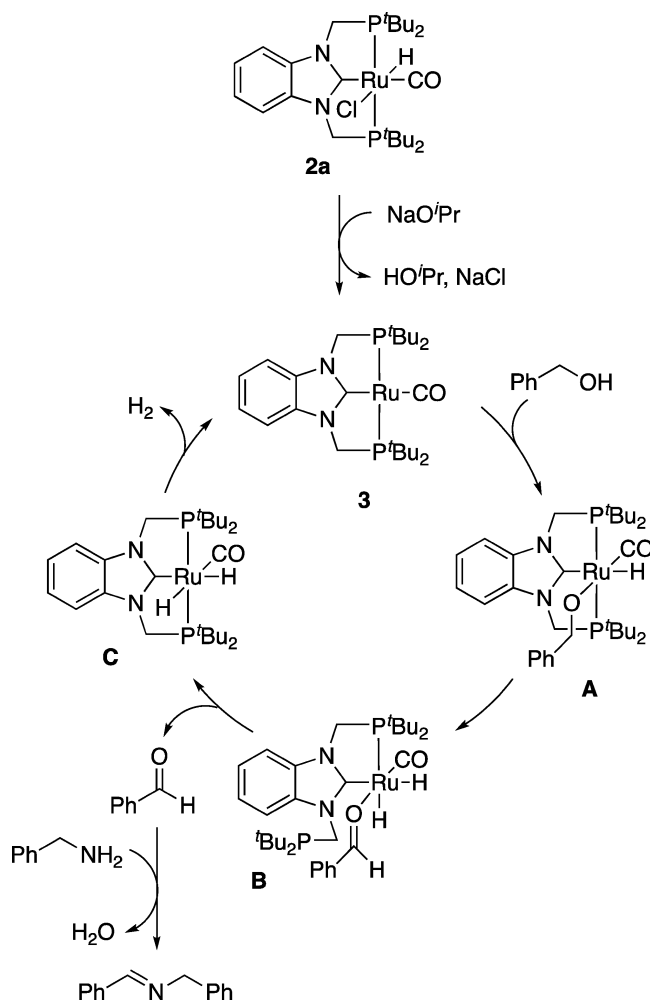
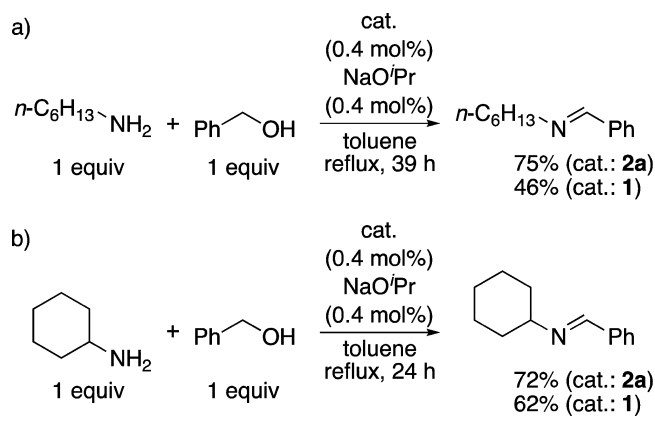


**Figure 3.** Plausible reaction mechanism for direct synthesis of imine from benzyl alcohol and benzylamine catalyzed by ruthenium-PCP[1] complex **2a**.

benzaldehyde from **B** gives the corresponding ruthenium-dihydride complex (**C**). Finally, reductive elimination of two hydride ligands from **C** generates the original square-planar ruthenium(0) complex **3** together with hydrogen gas. The produced benzaldehyde reacts with 1 equiv of benzylamine to give the final product *N*-benzylidenebenzylamine. Separately, we detected hydrogen gas after the catalytic reaction in a

closed system at a lower temperature of 80 °C. This experimental result supports our proposal shown in Figure 3.

Previously, Milstein and co-workers proposed that unsaturated amide complex **6** via deprotonation of [RuHCl(CO)-(PNP)] **1** promotes direct synthesis of imines from reactions of amines with alcohols. In sharp contrast to the proposal by Milstein and co-workers, we have found that unsaturated complex **3** via deprotonation of **2a** may work as a key intermediate to promote the same transformation.<sup>17</sup> In the present reaction system, we believe that the strongly coordinating ability of the PCP-pincer ligand to the ruthenium center realizes longer lifetime of the catalytic activity of **2a** than that of **1**.

In summary, we have prepared ruthenium complexes bearing *N*-heterocyclic carbene- and phosphine-based PCP-type pincer ligands [RuHCl(CO)(PCP[1])] **2a** and [RuHCl(CO)-(PCP[2])] **2b**. Spectroscopic data indicated that ruthenium complex bearing a PCP[1] ligand **2a** has a stronger  $\pi$ -accepting character than ruthenium complex bearing a PCP[2] ligand **2b**. Both ruthenium complexes **2a** and **2b** worked as effective catalysts toward direct synthesis of imines from reactions of amines with benzyl alcohol. The lifetime of **2a** was longer than that of ruthenium complex bearing a PNP ligand [RuHCl(CO)(PNP)] **1**. Further study is currently in progress to prepare other transition metal complexes bearing the PCP-pincer ligands and to investigate their unique catalytic activity in detail.

## EXPERIMENTAL SECTION

**General Method.** <sup>1</sup>H NMR (270 MHz) and <sup>31</sup>P{<sup>1</sup>H} NMR (109 MHz) spectra were recorded on a JEOL Excalibur 270 spectrometer in suitable solvents, and spectra were referenced to the residual solvent (<sup>1</sup>H) or external standard (<sup>31</sup>P{<sup>1</sup>H}: 85% H<sub>3</sub>PO<sub>4</sub>). IR spectra were recorded on a JASCO FT/IR 4100 Fourier transform infrared spectrometer. Elemental analyses were performed at the Micro-analytical Center of The University of Tokyo. Evolved dihydrogen was quantified by a gas chromatography using a Shimadzu GC-8A with a TCD detector and a SHINCARBON ST (6 m × 3 mm).

All manipulations were carried out under an atmosphere of nitrogen or argon by using standard Schlenk techniques or glovebox techniques unless otherwise stated. Solvents were dried by the usual methods and then distilled and degassed before use. PCP[1]HPF<sub>6</sub>,<sup>10</sup> PCP[2]HCl,<sup>10</sup> and [RuHCl(CO)(PPh<sub>3</sub>)<sub>3</sub>]<sup>18</sup> were prepared according to the literature methods.

**Synthesis of [RuHCl(CO)(PNP)] (1).** Complex **1** was prepared by the literature method.<sup>4c</sup> Crystals suitable for X-ray crystallographic analysis were prepared by recrystallization from THF–hexane.

**Synthesis of [RuHCl(CO)(PCP[1])] (2a).** To a suspension of PCP[1]HPF<sub>6</sub> (407 mg, 0.702 mmol) in toluene (20 mL) was added KN(SiMe<sub>3</sub>)<sub>2</sub> (197 mg, 0.985 mmol), and the mixture was stirred at room temperature for 1 h. The suspension was filtered through Celite. The filtrate was added to a suspension of [RuHCl(CO)(PPh<sub>3</sub>)<sub>3</sub>] (668 mg, 0.701 mmol) in toluene (15 mL) and stirred at 65 °C for 21 h. The solvent was removed under vacuum. The residue was dissolved in THF (7 mL), hexane (50 mL) was added, and the suspension was filtered. The resulting solid was washed with hexane (10 mL × 3) and recrystallized from CH<sub>2</sub>Cl<sub>2</sub>–hexane to obtain [RuHCl(CO)-(PCP[1])] as orange crystals (222 mg, 0.370 mmol, 53%). <sup>1</sup>H NMR (C<sub>6</sub>D<sub>6</sub>):  $\delta$  = 16.84 (t, *J* = 19.2 Hz, 1H, RuH), 1.08 (pseudo t, *J* = 6.4 Hz, 18H, P<sup>*t*</sup>Bu<sub>2</sub>), 1.53 (pseudo t, *J* = 6.4 Hz, 18H, P<sup>*t*</sup>Bu<sub>2</sub>), 3.88 (dt, *J* = 2.4 and 12.3 Hz, 2H, NCH<sub>2</sub>P), 4.25 (d, *J* = 12.3 Hz, 2H, NCH<sub>2</sub>P), 6.79–6.82 (m, 2H, ArH), 6.98–7.01 (m, 2H, ArH). <sup>31</sup>P{<sup>1</sup>H} NMR (C<sub>6</sub>D<sub>6</sub>):  $\delta$  103.2 (s, <sup>*t*</sup>Bu<sub>2</sub>P). IR (KBr, cm<sup>-1</sup>): 1937 ( $\nu_{\text{CO}}$ ), 2109 ( $\nu_{\text{RuH}}$ ). Anal. Calcd for C<sub>26</sub>H<sub>45</sub>ClN<sub>2</sub>OP<sub>2</sub>Ru: C, 52.04; H, 7.56; N, 4.67. Found: C, 51.71; H, 7.48; N, 4.79.

**Synthesis of [RuHCl(CO)(PCP[2])] (2b).** To a suspension of PCP[2]HCl (183 mg, 0.407 mmol) in toluene (18 mL) was added KN(SiMe<sub>3</sub>)<sub>2</sub> (112 mg, 0.561 mmol), and the mixture was stirred at room temperature for 2 h. The suspension was filtered through Celite. The filtrate was added to a suspension of [RuHCl(CO)(PPh<sub>3</sub>)<sub>3</sub>] (311 mg, 0.327 mmol) in toluene (7 mL) and stirred at 70 °C for 2 h. The solvent was removed under vacuum. The residue was washed with THF/hexane (1/5 v/v, 12 mL × 2) and hexane (5 mL × 2) to obtain [RuHCl(CO)(PCP[2])] as a gray solid (67.6 mg, 0.117 mmol, 36%). Analytically pure sample was prepared by slow evaporation from THF. Crystals suitable for X-ray analysis were prepared by recrystallization from CH<sub>2</sub>Cl<sub>2</sub>–hexane. The NMR spectrum was recorded on a JEOL JNM-ECS 400 spectrometer. <sup>1</sup>H NMR (THF-*d*<sub>8</sub>, 400 MHz): δ –17.43 (t, *J* = 20.0 Hz, 1H, RuH), 1.14 (pseudo t, *J* = 6.1 Hz, 18H, P<sup>*t*</sup>Bu<sub>2</sub>), 1.40 (pseudo t, *J* = 6.1 Hz, 18H, P<sup>*t*</sup>Bu<sub>2</sub>), 1.89–2.00 (m, 4H, CH<sub>2</sub>), 3.83–3.94 (m, 2H, CH<sub>2</sub>), 5.25 (br s, 2H, CH<sub>2</sub>), 6.98 (s, 2H, CH=CH). <sup>31</sup>P{<sup>1</sup>H} NMR (THF-*d*<sub>8</sub>, 162 MHz): δ 64.5 (s, <sup>*t*</sup>Bu<sub>2</sub>P). IR (KBr, cm<sup>-1</sup>): 1907 (ν<sub>CO</sub>), 2046 (ν<sub>RuH</sub>). Anal. Calcd for C<sub>24</sub>H<sub>47</sub>ClN<sub>2</sub>O<sub>2</sub>P<sub>2</sub>Ru: C, 49.86; H, 8.19; N, 4.85. Found: C, 49.69; H, 8.28; N, 5.23.

**Generation of [Ru(CO)(PCP[1])] (3).** To a solution of [RuHCl(CO)(PCP[1])] (2a; 12 mg, 0.02 mmol) in THF-*d*<sub>8</sub> (0.75 mL) was added a solution of lithium diisopropylamide (1.0 M in THF, 40 μL, 0.040 mmol) and stirred at room temperature for 7 h. The product was too unstable to be isolated. <sup>1</sup>H NMR (THF-*d*<sub>8</sub>): δ 1.37 (pseudo t, *J* = 6.3 Hz, 36H, <sup>*t*</sup>Bu<sub>2</sub>P), 4.12 (s, 4H, NCH<sub>2</sub>P), 7.04–7.08 (m, 2H, ArH), 7.16–7.19 (m, 2H, ArH). <sup>31</sup>P{<sup>1</sup>H} NMR (THF-*d*<sub>8</sub>): δ 115.6 (s, <sup>*t*</sup>Bu<sub>2</sub>P). IR (THF, cm<sup>-1</sup>): 1845 (ν<sub>CO</sub>).

**Typical Procedure for Catalytic Synthesis of *N*-Benzylidenebenzylamines.** To a mixture of 2a (12 mg, 0.02 mmol) and NaO<sup>*t*</sup>Pr (1.6 mg, 0.02 mmol) in toluene (1 mL) were added benzyl alcohol (0.52 mL, 5.02 mmol) and benzylamine (0.55 mL, 5.04 mmol), and the mixture was refluxed for 24 h. After cooling, the amount of *N*-benzylidenebenzylamine was analyzed with <sup>1</sup>H NMR by using hexamethylbenzene as an internal standard.

**X-ray Crystallography.** Diffraction data for 1, 2a, and 2b were collected for the 2θ range of 5–55° at –100 °C (for 1 and 2b) or –150 °C (for 2a) on a Rigaku RAXIS RAPID imaging plate area detector with graphite-monochromated Mo Kα radiation (λ = 0.71075 Å), with VariMax optics. Intensity data were corrected for Lorentz-polarization effects and for empirical absorption (ABSCOR). The structure solution and refinements were carried out using the CrystalStructure crystallographic software package.<sup>19</sup> The positions of the non-hydrogen atoms were determined by direct methods (SIR 97<sup>20</sup>) and subsequent Fourier syntheses (SHELXL version 2016/6<sup>21</sup>) and were refined on Fo<sup>2</sup> using all unique reflections by full-matrix least-squares with anisotropic thermal parameters. All the hydrogen atoms except for H(1) atom of 1 were placed at the calculated positions with fixed isotropic parameters, while positions of some hydrogen atoms could not be refined.

For the crystal of 2a, the molecule of 2a contains whole-molecule disorder where the central ruthenium atom and its surrounding ligands may be disordered among more than two positions but was solved modeling over two positions (Ru(1)–Cl(1) and Ru(2)–Cl(2)) with atom occupancies of 0.9 and 0.1, respectively, while positions of six hydrogen atoms bonded to two carbon atoms (C(17) and C(24)) close to the Cl(2) atom could not be refined. The hydrido ligand on the ruthenium atom was not placed.

For the crystal of 2b, the unit cell contains a solvent accessible void of 729 Å<sup>3</sup>. The <sup>1</sup>H NMR suggested that the void was occupied with dichloromethane molecules, which could not be located appropriately. The diffused electron density associated with the solvent molecule was removed by SQUEEZE routine in PLATON.<sup>22</sup> The hydrido ligand on the ruthenium atom was not placed.

## ■ ASSOCIATED CONTENT

### Supporting Information

The Supporting Information is available free of charge on the ACS Publications website at DOI: 10.1021/acs.organomet.8b00465.

Crystal data including bond lengths and angles for compounds 1, 2a, and 2b (PDF)

### Accession Codes

CCDC 1825365, 1847881, and 1849515 contain the supplementary crystallographic data for this paper. These data can be obtained free of charge via [www.ccdc.cam.ac.uk/data\\_request/cif](http://www.ccdc.cam.ac.uk/data_request/cif), or by emailing [data\\_request@ccdc.cam.ac.uk](mailto:data_request@ccdc.cam.ac.uk), or by contacting The Cambridge Crystallographic Data Centre, 12 Union Road, Cambridge CB2 1EZ, UK; fax: +44 1223 336033.

## ■ AUTHOR INFORMATION

### Corresponding Author

\*E-mail: [ynishiba@sys.t.u-tokyo.ac.jp](mailto:ynishiba@sys.t.u-tokyo.ac.jp).

### ORCID

Aya Eizawa: 0000-0001-6713-1871

Kazunari Nakajima: 0000-0001-9892-5877

Yoshiaki Nishibayashi: 0000-0001-9739-9588

### Notes

The authors declare no competing financial interest.

## ■ ACKNOWLEDGMENTS

The present project is supported by CREST, JST (JPMJCR1541). We acknowledge Grants-in-Aid for Scientific Research (Nos. JP17H01201 and JP15H05798) from JSPS and MEXT. A.E. is a recipient of the JSPS Predoctoral Fellowships for Young Scientists. We also thank the Research Hub for Advanced Nano Characterization at The University of Tokyo for X-ray analysis.

## ■ REFERENCES

- (1) (a) *Organometallic Pincer Chemistry*; van Koten, G., Milstein, D., Eds.; Topics in Organometallic Chemistry; Springer-Verlag: Berlin, 2013. (b) Lawrence, M. A. W.; Green, K.-A.; Nelson, P. N.; Lorraine, S. C. Review: Pincer Ligands—Tunable, Versatile and Applicable. *Polyhedron* **2018**, *143*, 11–27.
- (2) Khusnutdinova, J. R.; Milstein, D. Metal–Ligand Cooperation. *Angew. Chem., Int. Ed.* **2015**, *54*, 12236–12273.
- (3) For recent reviews on ruthenium–pincer complexes, see: (a) Milstein, D. Discovery of Environmentally Benign Catalytic Reactions of Alcohols Catalyzed by Pyridine-Based Pincer Ru Complexes, Based on Metal–Ligand Cooperation. *Top. Catal.* **2010**, *53*, 915–923. (b) Gunanathan, C.; Milstein, D. Metal–Ligand Cooperation by Aromatization–dearomatization: A New Paradigm in Bond Activation and “Green” Catalysis. *Acc. Chem. Res.* **2011**, *44*, 588–602. (c) Gunanathan, C.; Milstein, D. Bond Activation and Catalysis by Ruthenium Pincer Complexes. *Chem. Rev.* **2014**, *114*, 12024–12087.
- (4) (a) Zhang, J.; Gandelman, M.; Shimon, L. J. W.; Rozenberg, H.; Milstein, D. Electron-Rich, Bulky Ruthenium PNP-Type Complexes. Acceptorless Catalytic Alcohol Dehydrogenation. *Organometallics* **2004**, *23*, 4026–4033. (b) Zhang, J.; Leitus, G.; Ben-David, Y.; Milstein, D. Facile Conversion of Alcohols into Esters and Dihydrogen Catalyzed by New Ruthenium Complexes. *J. Am. Chem. Soc.* **2005**, *127*, 10840–10841. (c) Gnanaprakasam, B.; Zhang, J.; Milstein, D. Direct Synthesis of Imines from Alcohols and Amines with Liberation of H<sub>2</sub>. *Angew. Chem., Int. Ed.* **2010**, *49*, 1468–1471. (d) Zhang, J.; Balaraman, E.; Leitus, G.; Milstein, D.

- Electron-Rich PNP- and PNN-Type Ruthenium(II) Hydrido Borohydride Pincer Complexes. Synthesis, Structure, and Catalytic Dehydrogenation of Alcohols and Hydrogenation of Esters. *Organometallics* **2011**, *30*, 5716–5724. (e) Gnanaprakasam, B.; Balaraman, E.; Ben-David, Y.; Milstein, D. Synthesis of Peptides and Pyrazines from  $\beta$ -Amino Alcohols through Extrusion of  $H_2$  Catalyzed by Ruthenium Pincer Complexes: Ligand-Controlled Selectivity. *Angew. Chem., Int. Ed.* **2011**, *50*, 12240–12244. (f) Montag, M.; Zhang, J.; Milstein, D. Aldehyde Binding through Reversible C–C Coupling with the Pincer Ligand upon Alcohol Dehydrogenation by a PNP–Ruthenium Catalyst. *J. Am. Chem. Soc.* **2012**, *134*, 10325–10328.
- (5) (a) Precht, M. H. G.; Wobser, K.; Theyssen, N.; Ben-David, Y.; Milstein, D.; Leitner, W. Direct Coupling of Alcohols to Form Esters and Amides with Evolution of  $H_2$  Using *in situ* Formed Ruthenium Catalysts. *Catal. Sci. Technol.* **2012**, *2*, 2039–2042. (b) Nielsen, M.; Kammer, A.; Cozzula, D.; Junge, H.; Gladiali, S.; Beller, M. Efficient Hydrogen Production from Alcohols under Mild Reaction Conditions. *Angew. Chem., Int. Ed.* **2011**, *50*, 9593–9597. (c) Nielsen, M.; Junge, H.; Kammer, A.; Beller, M. Towards a Green Process for Bulk–Scale Synthesis of Ethyl Acetate: Efficient Acceptorless Dehydrogenation of Ethanol. *Angew. Chem., Int. Ed.* **2012**, *51*, 5711–5713.
- (6) (a) Tanaka, R.; Yamashita, M.; Nozaki, K. Catalytic Hydrogenation of Carbon Dioxide Using Ir(III)–Pincer Complexes. *J. Am. Chem. Soc.* **2009**, *131*, 14168–14169. (b) Tanaka, R.; Yamashita, M.; Chung, L. W.; Morokuma, K.; Nozaki, K. Mechanistic Studies on the Reversible Hydrogenation of Carbon Dioxide Catalyzed by an Ir–PNP Complex. *Organometallics* **2011**, *30*, 6742–6750. (c) Aoki, W.; Watanavinin, N.; Kusumoto, S.; Nozaki, K. Development of Highly Active Ir–PNP Catalysts for Hydrogenation of Carbon Dioxide with Organic Bases. *Bull. Chem. Soc. Jpn.* **2016**, *89*, 113–124.
- (7) Obligation, J. V.; Semproni, S. P.; Chirik, P. J. Cobalt-Catalyzed C–H Borylation. *J. Am. Chem. Soc.* **2014**, *136*, 4133–4136.
- (8) For selected reviews, see: (a) *Nitrogen Fixation*; Nishibayashi, Y., Ed.; Topics in Organometallic Chemistry; Springer Nature: Cham, 2017. (b) Nishibayashi, Y. Recent Progress in Transition-Metal-Catalyzed Reduction of Molecular Dinitrogen under Ambient Reaction Conditions. *Inorg. Chem.* **2015**, *54*, 9234–9247. (c) Nishibayashi, Y. Development of Catalytic Nitrogen Fixation Using Transition Metal–Dinitrogen Complexes under Mild Reaction Conditions. *Dalton Trans.* **2018**, *47*, 11290–11297.
- (9) (a) Arashiba, K.; Miyake, Y.; Nishibayashi, Y. A Molybdenum Complex Bearing PNP-Type Pincer Ligands Leads to the Catalytic Reduction of Dinitrogen into Ammonia. *Nat. Chem.* **2011**, *3*, 120–125. (b) Kinoshita, E.; Arashiba, K.; Kuriyama, S.; Miyake, Y.; Shimazaki, R.; Nakanishi, H.; Nishibayashi, Y. Synthesis and Catalytic Activity of Molybdenum–Dinitrogen Complexes Bearing Unsymmetric PNP-Type Pincer Ligands. *Organometallics* **2012**, *31*, 8437–8443. (c) Kuriyama, S.; Arashiba, K.; Nakajima, K.; Tanaka, H.; Kamaru, N.; Yoshizawa, K.; Nishibayashi, Y. Catalytic Formation of Ammonia from Molecular Dinitrogen by Use of Dinitrogen-Bridged Dimolybdenum–Dinitrogen Complexes Bearing PNP-Pincer Ligands: Remarkable Effect of Substituent at PNP-Pincer Ligand. *J. Am. Chem. Soc.* **2014**, *136*, 9719–9731. (d) Tanaka, H.; Arashiba, K.; Kuriyama, S.; Sasada, A.; Nakajima, K.; Yoshizawa, K.; Nishibayashi, Y. Unique Behaviour of Dinitrogen-Bridged Dimolybdenum Complexes Bearing Pincer Ligand towards Catalytic Formation of Ammonia. *Nat. Commun.* **2014**, *5*, 3737. (e) Kuriyama, S.; Arashiba, K.; Nakajima, K.; Tanaka, H.; Yoshizawa, K.; Nishibayashi, Y. Nitrogen Fixation Catalyzed by Ferrocene-Substituted Dinitrogen-Bridged Dimolybdenum–Dinitrogen Complexes: Unique Behavior of Ferrocene Moiety as Redox Active Site. *Chem. Sci.* **2015**, *6*, 3940–3951. (f) Arashiba, K.; Eizawa, A.; Tanaka, H.; Nakajima, K.; Yoshizawa, K.; Nishibayashi, Y. Catalytic Nitrogen Fixation via Direct Cleavage of Nitrogen–Nitrogen Triple Bond of Molecular Dinitrogen under Ambient Reaction Conditions. *Bull. Chem. Soc. Jpn.* **2017**, *90*, 1111–1118.
- (10) Eizawa, A.; Arashiba, K.; Tanaka, H.; Kuriyama, S.; Matsuo, Y.; Nakajima, K.; Yoshizawa, K.; Nishibayashi, Y. Remarkable Catalytic Activity of Dinitrogen-Bridged Dimolybdenum Complexes Bearing NHC-Based PCP-Pincer Ligands toward Nitrogen Fixation. *Nat. Commun.* **2017**, *8*, 14874.
- (11) (a) Plikhta, A.; Pöthig, A.; Herdtweck, E.; Rieger, B. Toward New Organometallic Architectures: Synthesis of Carbene-Centered Rhodium and Palladium Bisphosphine Complexes. Stability and Reactivity of  $[PC^{Bim}PRh(L)][PF_6]$  Pincers. *Inorg. Chem.* **2015**, *54*, 9517–9528. (b) Gradert, C.; Stucke, N.; Krahmer, J.; Näther, C.; Tuzcek, F. Molybdenum Complexes Supported by Mixed NHC/Phosphine Ligands: Activation of  $N_2$  and Reaction With  $P(OMe)_3$  to the First Meta-Phosphite Complex. *Chem. - Eur. J.* **2015**, *21*, 1130–1137.
- (12) For selected reviews on NHCs, see: (a) Herrmann, W. A.; Köcher, C. N-Heterocyclic Carbenes. *Angew. Chem., Int. Ed. Engl.* **1997**, *36*, 2162–2187. (b) Herrmann, W. A. N-Heterocyclic Carbenes: A New Concept in Organometallic Catalysis. *Angew. Chem., Int. Ed.* **2002**, *41*, 1290–1309. (c) Hahn, F. E.; Jahnke, M. C. Heterocyclic Carbenes: Synthesis and Coordination Chemistry. *Angew. Chem., Int. Ed.* **2008**, *47*, 3122–3172. (d) Díez-González, S.; Marion, N.; Nolan, S. P. N-Heterocyclic Carbenes in Late Transition Metal Catalysis. *Chem. Rev.* **2009**, *109*, 3612–3676. (e) de Frémont, P.; Marion, N.; Nolan, S. P. Carbenes: Synthesis, Properties, and Organometallic Chemistry. *Coord. Chem. Rev.* **2009**, *253*, 862–892. (f) Benhamou, L.; Chardon, E.; Lavigne, G.; Bellemin-Lapponnaz, S.; César, V. Synthetic Routes to N-Heterocyclic Carbene Precursors. *Chem. Rev.* **2011**, *111*, 2705–2733. (g) Hopkinson, M. N.; Richter, C.; Schedler, M.; Glorius, F. An Overview of N-Heterocyclic Carbenes. *Nature* **2014**, *510*, 485–496. (h) *N-Heterocyclic Carbenes*; Nolan, S. P., Ed.; Wiley-VCH: Weinheim, 2014.
- (13) (a) Matoba, K.; Eizawa, A.; Nishimura, S.; Arashiba, K.; Nakajima, K.; Nishibayashi, Y. Practical Synthesis of a PCP-Type Pincer Ligand and Its Metal Complexes. *Synthesis* **2018**, *50*, 1015–1019. (b) Takaoka, S.; Eizawa, A.; Kusumoto, S.; Nakajima, K.; Nishibayashi, Y.; Nozaki, K. Hydrogenation of Carbon Dioxide with Organic Base by  $PC^{11}P$ -Ir Catalysts. *Organometallics* **2018**, DOI: 10.1021/acs.organomet.8b00377.
- (14) Gusev, D. G. Electronic and Steric Parameters of 76 N-Heterocyclic Carbenes in  $Ni(CO)_3(NHC)$ . *Organometallics* **2009**, *28*, 6458–6461.
- (15) Tanabe, Y.; Kuriyama, S.; Arashiba, K.; Nakajima, K.; Nishibayashi, Y. Synthesis and Reactivity of Ruthenium Complexes Bearing Arsenic-Containing Arsenic-Nitrogen-Arsenic-Type Pincer Ligand. *Organometallics* **2014**, *33*, 5295–5300.
- (16) Salem, H.; Shimon, L. J. W.; Diskin-Posner, Y.; Leitner, G.; Ben-David, Y.; Milstein, D. Formation of Stable *trans*-Dihydride Ruthenium(II) and 16-Electron Ruthenium(0) Complexes Based on Phosphinite PONOP Pincer Ligands. Reactivity toward Water and Electrophiles. *Organometallics* **2009**, *28*, 4791–4806.
- (17) Goni, M. A.; Rosenberg, E.; Gobetto, R.; Chierotti, M. Dehydrogenative Coupling of Alcohols to Esters on a Silica Polyamine Composite by Immobilized PNN and PONOP Pincer Complexes of Ruthenium. *J. Organomet. Chem.* **2017**, *845*, 213–228.
- (18) Boniface, S. M.; Clark, G. R.; Collins, T. J.; Roper, W. R. Preparation of Octahedral Hydrido-aquo-Ruthenium(II) Complexes, and Structural Characterisation of Hydrido-aquodicyarbonylbis-(triphenylphosphine)-ruthenium(II) Tetrafluoroborate. *J. Organomet. Chem.* **1981**, *206*, 109–117.
- (19) *CrystalStructure 4.0: Single Crystal Structure Analysis Software*; MSC: The Woodlands, TX, 2010.
- (20) Altomare, A.; Burla, M. C.; Camalli, M.; Casciaro, G. L.; Giacovazzo, C.; Guagliardi, A.; Moliterni, A. G. G.; Polidori, G.; Spagna, R. SIR97: A New Tool for Crystal Structure Determination and Refinement. *J. Appl. Crystallogr.* **1999**, *32*, 115–119.
- (21) Sheldrick, G. M. A Short History of SHELX. *Acta Crystallogr., Sect. A: Found. Crystallogr.* **2008**, *64*, 112–122.
- (22) Spek, A. L. *PLATON: A Multipurpose Crystallographic Tool*; Utrecht University: Utrecht, The Netherlands, 1998.